European Rotorcraft Forum

Encountering Helicopter Wake by Light Aircraft

Yaxing Wang, Mark White and George N. Barakos

School of Engineering, University of Liverpool, L69 3GH, U.K.
Email: yxwang@liverpool.ac.uk

Peter Tormey and Panagiota Pantazopoulou

Civil Aviation Authority, U.K.

Abstract

The wake generated by a helicopter is different to that of a fixed-wing aircraft. Rotorcraft wake vortices are more intense and have their own characteristics in terms of structure, duration and decay. A number of serious and fatal accidents have happened when light aircraft have entered into a helicopter wake and the pilots have lost control. These accidents often happen near airports where helicopters are in a hover taxi and the encountering aircraft is in a landing or departure procedure, which means that both the helicopter and the aircraft are at low altitude and at relatively low speed. This type of wake encounter scenario has its own specific features. In this paper, three different methods of modelling helicopter wakes: prescribed wake, free wake and the CFD actuator disk, are presented and have been validated with available wind tunnel and flight test data. The free wake model was then selected to generate the wake vortices of a helicopter hover taxing over an airport runway. The Beddoes wake model with wake decay laws were then used to generate the far wake of a helicopter in level flight. The wake induced velocity flow fields were integrated into an aircraft flight dynamics model and piloted flight simulations were carried out to study a light aircraft encounter during landing and level flight with a helicopter wake. Wake encounter parameters of helicopter height, forward speed, orientation angle and offset to the runway centerline were considered in the simulations. For each wake encounter case, the pilot's subjective assessment of the severity and the objective aircraft's dynamic responses were recorded. It was found that for the current landing wake encounter scenario, the existing criteria of hazardous distance might not be suitable because the wake encounter occurs close to the ground. The landing simulation results suggest that for a helicopter in low speed (less than 40 kt) hover-taxing, the wake encounter detectable horizontal distance is about three times the diameter of the rotor, which coincides with the current safety guideline of Civil Aviation Authority. The simulations reveal that the parameters of helicopter height and speed, encountering angle and offset from the runway centreline all have impacts on the level of hazard of an encounter and the pilot's wake encounter severity ratings. The level flight simulations indicate that the wake still affects the encountering aircraft when it is flying below the helicopter at a vertical distance up to two times of rotor diameter, and it is found that at the simulated helicopter forward speed, the wake caused upsets reduce to a insignificant level after the wake is decayed to 50% of its original strength.

1 INTRODUCTION

The wakes of fixed-wing aircraft and helicopters are studied in aviation and one of the areas of interest is the investigation of the separation distance or separation time criteria used for wake encounter. There are clear definitions of the separation time or distance for the wake encounter between fixed-wing aircraft [3, 14]. However, for the wake encounter between a wake generating helicopter and an encountering light aircraft, the separation distance is not clearly defined and lacks of details. There is some guidance for helicopter wake encounters, for example, the three-rotor-diameter separation distance described in the CAP 493, Manual of Air traffic Services [3].

Serious and fatal accidents have happened when a light aircraft has encountered a helicopter wake and downwash and the pilot has lost control [2, 15]. The wake generated by a helicopter is different to that of a fixed-wing aircraft; helicopter wake vortices are more intense with different flow structure, duration and decay. Helicopter wake vortices depend on the type of the helicopter (weight, size, and configuration) and its operating conditions (altitude, speed). Helicopter wake encounter accidents have happened around airports where a helicopter is in a hover or hover taxi regime and the light aircraft is undergoing a landing or departure procedure. In either case, both the helicopter and the aircraft are at low altitudes and relatively low speeds. This type of wake encounter scenario has its own distinct features. When a helicopter is flying at low altitude, ground effect can distort its wake vortices and a low forward speed causes a large wake skew angle. All these features are different to that of the available helicopter fly-by LIDAR measurement wake data [7, 13] where the helicopter was flying at higher altitudes and larger forward speeds. For a landing aircraft, because it is close to ground, even a small wake upset could cause a severe hazard. In this circumstance, the current wake encounter criteria might not be suitable. Flight probe tests and fly-by measurement data for a landing aircraft encountering a helicopter wake are scarce and are difficult to conduct.

Doppler LIDAR was used by Kopp [7] to measure the wake vortices generated by military aircraft and rotorcraft. The measurements were mainly focused on the roll-up phase of the vortices. One of the fly-by LIDAR measurements ob-

tained was for the wake of a Puma helicopter. The tangential velocity profiles of the port vortices at two time instances and the decay of the maximum tangential velocity were presented. These data provided reference sources for the validation of various wake models. Another flight test investigation of rotorcraft wake vortices in forward flight was carried out by Teager etc. [13]. Different rotorcraft were used in their tests. Wake vortex strength and decay characteristics were calculated from the LIDAR measurements. The detectability and hazard distances for small aircraft behind helicopter were established based on the flight test data. However, all their LDV measurements were for helicopter airspeeds above 40 knots.

Wind turbines near airports, either isolated or in a cluster as a wind farm, could also generate wakes and affect nearby aircraft. There is limited guidance or criteria for the wind turbine wake hazards. Furthermore, LIDAR data for wind turbine is scarce.

Flight simulation can play an important role in the prediction and assessment of wake encounter hazards. It is a safe, low cost and controllable method of investigation. However, wake encounter simulation has its own requirements in order to be a useful tool. An accurate wake model is essential for the generation of wake velocity data. In addition, a validated aircraft flight dynamic model is necessary and the wake velocity data has to be carefully integrated into the simulation system to account for the interference of the wake on the aircraft flight dynamics when a wake encounter occurs. Piloted simulation trials are needed to assess the severity of wake encounter, whilst a high level of fidelity of the visual cues is also very important to reflect the real wake encounter scene.

The objectives of the work presented in this paper were: (1) Study and validation of different numerical models to generate helicopter rotor wake, from relatively simple prescribed wake models to free wake models and finally more complex CFD based modelling. (2) Use the selected wake model to calculate the wake induced velocity field from a rotorcraft and integrate it into an aircraft flight dynamics model to carry out piloted wake encounter simulation trials in a flight simulator.

The aim of the flight simulation testing is to answer the following questions:

- What level of disturbances can a helicopter wake cause on an approaching light aircraft?
- What differences do the helicopter parameters of height and speed have on the hazard of an encounter?
- How does the manner in which the wake is encountered i.e. encounter angle and offset between the helicopter and the aircraft change the aircraft hazard upset and hence the safety?

In this paper, three helicopter wake models are presented together with their validation against wind tunnel measurements. The wake encounter simulation set-up, test conditions and parameters are then described, followed by the results of the simulation trials and the conclusions.

2 HELICOPTER WAKE MODELLING

Accurate prediction and simulation of helicopter rotor wakes, including wake vortex geometry, wake age and wake induced velocity flow-fields, are vital to wake encounter simulation research. There are various helicopter wake models available in the literature [8] with different levels of complexity and fidelity. Three wake modelling methods are used in this study. These are prescribed wake models, free wake models and a CFD actuator disk model. These models are described in following sections.

2.1 Prescribed wake model

Prescribed wake models [1, 8] have been developed to enable predictions of the inflow characteristics through the rotor disk. These models prescribe the locations of the rotor tip vortices as functions of wake age on the basis of experimental observations. For hovering flight, the Landgrebe and Kocurek and Tangler models are widely used [8]. The Beddoes generalised wake model is commonly used for forward flight [1, 8]. The basic premise behind the Beddoes model is that the lateral and longitudinal distortions from a helical sweep in an actual rotor are small in comparison to the vertical distortions. These distortions can then be related to the velocity distribution on the rotor blade. The prescription of the vertical displacement of the tip vortices is related to empirical or semi-empirical weighting functions. Beddoes prescribed wake model was formulated for this study to calculate the vortex core positions and the induced velocity field was estimated using the Biot-Savart law. The wake vortices modelled by Beddoes prescribed model on a 4 blades rotor at 0.1 forward advance ratio is shown in figure 1.

2.2 Free wake model

In the free wake model [8, 9], the initial geometry of wake vortex is assumed. The wake is represented by a large number of discrete vortex elements. These vortex elements can propagate freely in the induced velocity field. In principle it does not require experimental results for formulation. A free wake model has been developed in this study to account for the ground effect and to produce more realistic vortex strength and hence the induced downwash velocity vectors for the simulation. The influence of ground effect is one of the most important factors that have to be considered when simulating helicopter flight near the ground in a hover taxi. In this wake model, the rotor blade is represented by a line vortex from root to tip and root vortex effects are ignored. The total rotor lift is assumed to be equal to the weight of helicopter and the circulation of the wake vortex equals the circulation of the blade it is shed off. The self-induced flow and the local wake curvature, as well as the effect of helicopter fuselage are considered in the formulation. Velocity field is estimated using the Biot-Savart law after the wake geometry is established. Figure 1 shows the iso-surface plot of vorticity, which indicates the geometry of vortex core, generated by the free wake model.

2.3 CFD actuator disk model

In a CFD actuator disk model, Navier-Stokes equations are solved with turbulence models to simulate the flow field. The helicopter rotor is simulated by an actuator disk, which is added into CFD domain as a momentum source to simulate

a pressure jump over the rotor. In this study the actuator disk method is implemented using the HMB flow solver [12] developed at University of Liverpool. The solver uses a cell-centred finite volume approach combined with an implicit dual-time method. Osher's upwind scheme is used to resolve the convective fluxes. Central differencing spatial discretisation method is used to solve the viscous terms. The non-linear system of equations that is generated as a result of the linearisation is then solved by integration in pseudo-time using a first-order backward difference. A Generalised Conjugate Gradient (GCG) method is then used in conjunction with a Block Incomplete Lower-Upper (BILU) factorisation as a pre-conditioner to solve the linear system of equations, which is obtained from a linearisation in pseudo-time. The flow solver can be used in serial or parallel mode [12].

For the CFD actuator disk model, the mesh and blocks were generated using ICEMCFD tool. A drum was created to enclose the actuator disk and sliding planes [12] were used to account for relative motion. The wake generated by the CFD actuator disk is shown in figure 1, where the stream-trace plots are used to illustrate the wake geometry.

3 VALIDATION OF THE WAKE MODELS

Heyson [5] measured the induced velocity fields near a lifting rotor in the Langley full-scale wind tunnel. The teetering type rotor consists of two untwisted blades with NACA 0012 aerofoil section. The rotor radius is 7.5 ft and the tip speed is 500 ft/s. His experimental data included the velocity fields at several downstream positions of the rotor. The wind tunnel test set-up and the measured velocity planes are shown in figure 2. The Beddoes prescribed model, the free wake model and the CFD actuator disk model have been applied using Heyson's test conditions and rotor parameters to simulate the rotor wake. In wake encounter study, the main concern is focused on the wake in the downstream region (mid and far wake) of the rotor. Comparisons of these modelling results with Heyson's wind tunnel test data are shown in figures 3, where the velocities at 2 transverse planes (yz plane) of x/R=2 and x/R=3 (downstream) are compared. At x/R=2, all three models showed reasonable accuracy in the vertical planes until z/R=0.5. Further away from the rotor, where the induced velocity was lower, the Beddoes and free wake models over-predicted the velocity. The CFD actuator disk model still predicted well in the inboard region but large discrepancy was shown in the outboard area, particularly around the two shoulders. In the further downstream region of x/R=3, where the tip vortices have been rolled up, the agreement is improved. The velocity was well predicted by the three models in the vertical planes up to z/R=0.7. Generally speaking, the CFD actuator disk model showed the best predictions among the three wake models but with the highest computational cost.

Fly-by Doppler LIDAR measurements of a Puma helicopter wake was presented by Kopp [7]. The tangential velocity of the port-side vortices were measured at the time about 9 seconds after their generation. The Puma helicopter forward velocity was 65 kts so the measurement position was about 20 rotor diameter downstream from the rotor center. This is in the very far wake range. Far wake or long age wake CFD simulation is a significant challenge as it requires high density grids and needs to overcome numerical dissipation [6]. A CFD actuator disk model and a Beddoes model have been applied to the Puma flight condition of Kopp's fly-by test. The measured maximum velocity decay over a long wake age was also presented which is reproduced in figure 4. The wake vortex decay is indicated by the decrease of the maximum tangential velocity measured near the port vortex core over the different passing-by time. During the first 10 seconds, the vortex maintains its strength almost constantly, which is followed by a near linear decay after 10 seconds. From this decay relation, the velocity magnitudes can be deduced at different ages or downstream distances. Comparisons of tangential velocity distributions of the actuator disk model are shown in figure 5, where the results of different CFD grid densities are plotted together to reveal the grid sensitivity. The finest grid (22 million cells) produced a reasonably good agreement with the fly-by test data in the far downstream region up to 6 rotor diameter from the rotor center. Further downstream wake CFD simulation needs to increase grid density tremendously which is not regarded to be a viable method to generate wake data for the proposed flight simulation.

The Beddoes model was developed mainly from the near wake wind tunnel measurements and there is no wake decay in the Beddoes model. In order to extend it to the far wake, the above mentioned wake decay relation was adopted to the Beddoes wake model to produce wake at long wake age. The results are shown in figure 5, where the tangential velocity distributions at different downstream positions are presented. At the far downstream position of 20D from the rotor, the velocity magnitude and distribution were predicted well.

4 INDUCED VELOCITY FLOW FIELD

The free wake model was selected to generate the helicopter wake data for the wake encounter simulation after considering the accuracy and computational cost of the three wake models. A Dauphin helicopter configuration was used in the wake encounter simulation. The free wake model was applied to the Dauphin helicopter rotor. The wake induced velocity vectors were calculated from the Biot-Savart law after the wake vortex elements were determined from the free wake model. The rotor hub is set at origin (0, 0, 0) along a runway centreline over the runway threshold. The induced velocity field covers a box of x =-20 ft to 320 ft (about 8 rotor diameter), y= -50 ft to 50 ft and z=-50 ft to 30 ft. The induced velocity field at different advance ratios of Dauphin helicopter can be seen in figure 6, where the wake geometry and three planes of velocity vectors and downwash contours at 0 (the rotor hub centre), 1D and 3D in downstream are displayed.

The oblique wake encounter is indicated in figure 7, where the helicopter orientation angle is set to 45^o and the helicopter rotor hub is also offset 2 rotor diameter from the runway centreline. The wake induced velocity field of Dauphin helicopter at a lower height (20 ft) is also illustrated in figure 7. In this case, the ground effect is more pronounced.

The Beddoes wake model with the measured wake decay relation was also applied on the Dauphin helicopter rotor to generate the far wake flow fields. The induced flow flow fields and the wake geometry are shown in figure 8 for the baseline

wake (no decay) and the wake with a 50% decay.

5 WAKE ENCOUNTER FLIGHT SIMULATION

The piloted wake encounter flight simulations were carried out in the HELIFLIGHT simulator [11] at the University of Liverpool by two test pilots. The wake encountering aircraft is a GA training aircraft configured to be similar to a Grob Tutor light aircraft. During the simulation the rolling/pitching moments, aircraft altitude change, velocities and accelerations during an encounter were recorded together with the pilot's control inputs to capture a complete description of the encounter. This data provided a quantitative measure of the effect of the wake on the aircraft. After each set of runs the pilot was asked to rate the hazard using the Wake Vortex Severity Rating Scale [10].

5.1 Wake encounter Scenarios

The first scenario was designed for helicopter wake encounters during approach landing as shown in figures 9, where the Dauphin helicopter is positioned offset the central line of the runway near the runway threshold when the GA aircraft is approaching to land. The response of the aircraft to the wake and the perceived hazard of the pilot to the encounter were measured for different advance ratios, orientation angles and encounter heights at the max rotor thrust coefficient. The wake of the helicopter was placed at the position on the runway that caused the aircraft to fly through it whilst on a standard approach profile, see figure 10. The Dauphin is a conventional configuration helicopter in the light category. At its maximum takeoff weight for the generation of the rotor wake, a thrust coefficient of 0.013 was estimated. For a helicopter hover taxing around a runway, the forward speed is normally low, hence three different rotorcraft speeds of 0 (hover), 20 kts, and 40 kts were chosen. The corresponding advance ratios are 0.0 (hover), 0.05 and 0.1. The helicopter was positioned at two heights of 50 ft and 20 ft and the orientation of the wake was adjusted by varying the angle of the wake to the runway and its lateral offset from the runway axis. The different wake angles caused the aircraft to encounter the wake at oblique angles whilst the offset causes interactions of the aircraft lifting surfaces with the wake at different stages of wake evolution.

The second scenario is designed for helicopter wake encounter during level flight. In this case, the Dauphin helicopter was positioned at a height of 200 ft and was at a forward speed of 65 kt (advance ratio of 0.15). The GA aircraft was flown behind the helicopter to penetrate the helicopter wake at different altitudes to investigate the effects of the vertical distance between the helicopter and the encountering aircraft. The wake induced velocities at 100% (baseline), 90%, 75% and 50% of wake strengths were used in the simulations to study the effects of the wake age or decay. In each run the pilot was asked to fly into the wake at a specific height level.

5.2 Simulator, aircraft flight dynamics model and pilot rating scale

The simulator used in the trials is the HELIFLIGHT simulator (shown in figure 9). It is a full motion simulator with a single-seat cockpit. There are 3 channels collimated visual displays for the Out-the-Window view and two chin-window displays. Pilot controls are provided by a four-axis dynamic control loading system. It has a six DOF full motion platform and the pilot is able to communicate with the control room at all times via a headset.

The aircraft flight dynamics model was developed in the FLIGHTLAB simulation package based on a Grob Tutor configuration. The main aircraft components of wing, fuselage, propeller, tail, fin, landing gears, engine and control system are modelled. Wake interference on the aircraft is integrated into the dynamics model as velocity look-up tables. The wake has an impact on the wings, fuselage, propellers, tail, fin and lift-surfaces.

During the trials, the pilot was asked to give feedback on the wake encounters and rate the severity according to a wake vortex encounter pilot rating scale, which is a scale that has been used in a previous study by Padfield et al [10]. The ratings scale is shown in figure 11. It provides a simple decision tree that enables the pilot to provide a subjective assessment of the level of wake encounter hazard.

5.3 Test procedure

For each test condition, the pilot was asked to fly the GA aircraft along a 3 degree glide slope path aimed to land the aircraft at a specified touchdown point for the landing scenario or to fly at a specific altitude for the level flight scenario. The wake was placed at a specific position according to the test matrix. The pilot was not informed whether the wake was present or not. In each simulation sortie, the pilot was asked to award the wake encounter severity ratings if the wake was detected. In addition to the rating, other parameters related to the aircraft dynamics, positions and pilot control activities were also recorded for further analysis. Generally, several runs of a same test condition were carried out to obtain consistent results prior to awarding of a wake vortex encounter rating.

6 SIMULATION RESULTS AND DISCUSSION

6.1 Helicopter wake encounter during landing

6.1.1 Vortex upset hazard

The helicopter wake vortex induced disturbances were probed by the GA light aircraft in the simulation to obtain a direct assessment of wake vortex hazard as a function of distance behind the wake generating helicopter. The size of the GA model is representative of small general aviation aircraft that are likely to be affected by rotorcraft wake vortices, whilst a Dauphin helicopter represents a typical small helicopter. In addition to the pilot's awarded wake encounter severity rating and comments, the aircraft dynamic response parameters can be used to assess the wake vortex upset hazard.

Criteria for test pilot assessments are dependent on the manner in which the assessment evolved [13]. For fixed wing aircraft encounters, generalised criteria to be used in approach to determine the limits of upsets (roll, pitch, yaw and any acceleration) which would permit continuation of the approaching rather than a go-around. The amount of control used and the most severe aircraft excursions which the pilots would tolerate need to be considered [13]. For a more definitive criterion, a rule of thumb has evolved that suggested that the maximum acceptable bank angle at published minimums would be that obtained by dividing 1200 by the wingspan in feet [13]. For the Boeing 747 it is 6 degrees of bank. For smaller aircraft like Grob Tutor (10 meter wing span), it is approximately 35 degree. Normally the hazardous roll angle limit was round off to 30 degree. The hazard distance was defined by Teager [13] as the distance at which a nominal 30 degree bank upset is caused.

In the helicopter wake encounter, the perceived severity of the hazard caused by the wake vortex on the encountering aircraft depends on the height and the speed of the helicopter and the vortex age, which is reflected in terms of the distance of the encounter behind the wake generating helicopter.

The time history plots of the aircraft responses and pilot control activities in a typical wake encounter case are shown in figure 12. The left-hand figures show the dynamic responses of aircraft attitude of roll, pitch and yaw angles, rates and accelerations. The pilot's control activities of the lateral, longitudinal sticks and the pedal, the altitude of the aircraft and the body accelerations in x, y and z body axes are plotted in the right hand column of figures. The aircraft encounters the wake at time about 47 second. The pilot gave this wake encounter an F rating for landing operation. The pilot commented that if the wake encounter was happened at a higher altitude, the rating would have been D.

In the current landing simulations, the GA aircraft bank angle did not exceed 30 degrees even for the most severely rated upset encounter. However, the test pilot gave an F rating for some of the encounters, which means, in his opinion, the safety of flight was compromised and the hazard is intolerable. The reason that the pilot gave such a rating is because during the phase of landing the aircraft is close to the ground, where there is little room to manoeuvre the aircraft even the vortex upset is small. The 30 degree bank angle criterion might not be well suitable to the wake encounter scenario during landing.

Another criterion for the wake encounter is the Vortex upset detectability distance at which the impact of the helicopter's wake vortex can be detected by the approaching aircraft. The data of the above test case are re-plotted in figure 13, where the X distance between the aircraft and the helicopter was used. The position of the three times of the rotor diameter was also indicated on the plots. The helicopter was positioned at the runway threshold (x=0) with a height of 50 ft. The GA aircraft approached landing on a 3 degree slope flight path. The roll acceleration and vertical (Z) body acceleration started to show abrupt changes at distance about 120 ft (about 3 diameter of the rotor) from the helicopter position. At a closer distance of about 80 ft (2D) the accelerations in pitch appeared. The peak of roll attitude rate is 21 degree/sec and peak roll angle is about 14 degree. A similar pitch rate appears later and the maximum pitch angle is 16 degree. A smaller yaw acceleration, yaw rate and yaw angle are also observed in the plots. The pilot applied lateral control to compensate the roll disturbance and later the longitudinal and pedal controls were also applied.

6.1.2 Helicopter speed or advance ratios

A higher advance ratio causes a smaller wake skew angle and the wake vortex moves faster to extend further downstream. Hence the wake vortex geometry is highly dependent on the advance ratio, so is the wake induced velocity distribution. Figure 14 shows the roll dynamic responses, vertical acceleration and lateral control input at the helicopter velocity of 0 (hover), 20 kt and 40 kt. The roll acceleration and rate plots indicated that the wake encounter detectability distances were at about 120ft (3D), 70ft (1.8D) and 30ft (0.8D) for the three speeds. Larger roll accelerations and rates were produced in the lower speed cases as the encounter occurred at a closer location to the helicopter. However, the largest roll angle, lateral control displacement and vertical body accelerations were generated at the highest velocity of 40 kt. The pilots awarded ratings of C and B to the hover and the 20 kt speed cases.

6.1.3 Effect of helicopter offset

When helicopter is re-located away from the centre line of the runway, the distance between the induced velocity calculation points and the wake vortex elements is increased. Dependent on the offset distance, in some regions of the box, the induced velocity would be reduced. It also might cause partially encounter, which means that only portion of the GA aircraft is affected by the wake. The offset effects are shown in figure 15, where the roll dynamic responses, lateral control inputs and vertical acceleration at three offsets are compared. The least upsets in the dynamic responses and lateral control inputs were generated at the 2D offset encounter and a rating of A was awarded, which indicated that the wake vortex was shifted away from the runway area and its effect was barely discernible. The upsets caused in the 1D offset case is still large due to the partial encounter and resulted in a C rating. The changes of the signs in the roll angle, the roll rate and acceleration and the lateral control indicate that the encounter character is different to that of the no offset encounter.

6.1.4 Wake encountering angles

Wake encounter angle changes the orientation between the wake vortex to the fixed induced velocity box. It is anticipated that the resulting wake induced velocity distribution would be altered when compared with the parallel (zero angle) encounter. The effects of the encounter angle are shown in figure 16, where the roll dynamic responses, lateral control and vertical acceleration are compared. The wakes were positioned at a offset of 1D from the runway centreline. The oblique encounters (45^o) caused the least upsets in the roll angle and the lateral control and a B rating was awarded. This is partly due to the fact that the wake vortex is skewed away from the centre line of the induced velocity box, which increased the distance between the vortex elements and the in-

duced velocity calculation points. This large distance reduces the induced velocity and hence generated less encounter upset. In the crossing encounter (90^o), the shortest detectability distance about 30 ft (0.75D) was found. The detectability distances were 120 ft (3D) and 90 ft (2.3D) for the parallel and the oblique encounters and a same C rating was awarded.

6.1.5 Helicopter height

For the landing wake encounter, simulation trials were also conducted at a lower helicopter height of 20 ft (0.5D). In this case the ground effect is expected to be more pronounced which would produced a different induced velocity field to the out ground effect cases. A comparison with the higher height case is shown in figure 17. The lower rotor caused similar levels of roll rate and acceleration on the encounter aircraft as that of the higher rotor. However, the maximum roll angle was significant smaller than that of the higher height case. A lower severity rating of B was awarded to the lower height case.

6.2 Helicopter wake encounter during level flight

6.2.1 Vortex upset hazard

The simulation results of helicopter wake encounter during level flight are shown in figure 18, where the time history plots of the aircraft responses and pilot control activities are presented. The GA aircraft flew into the wake at at the same level (altitude) as the helicopter. The figure indicated that the maximum disturbed roll angle of the GA aircraft was reached to 45 degree. The pilot applied up to 97% of the lateral control to compensate the the roll upset. The wake also caused a nearly 18 degree yaw displacement and up to 33% pedal was applied by the pilot. The roll rate and acceleration started at about 45.7 seconds, which corresponds to a distance of about 300 ft (7.5D) from the helicopter rotor center. The pilot rated this wake encounter severity as a G rating, which means that the excursion of aircraft states is such high that it causes marginal recovery and safe recovery cannot be assured.

6.2.2 Helicopter height and aircraft altitude

In the level fight simulation, the pilots were asked to fly the GA aircraft to penetrate the helicopter wake at different altitudes to investigate the effects of the vertical distance between the helicopter and the encountering aircraft. The wake is skewed when the helicopter is fly at a forward speed of 65 kt (μ=0.15). The wake induced velocity field is highly dependent not only the horizontal distance but also the vertical distance. The results are shown in figure 19. In the baseline case (200 ft), the GA was flying at the same height as the Dauphin helicopter and the wake caused the largest disturbances in the roll axis. The lower the altitude of the GA aircraft was, the less roll upsets were produced. The amounts of the control compensations were also reduced with the decrease of the altitude. At the altitude of 120 ft, the vertical distance between the helicopter and the GA aircraft is about 2D, the wake caused a maximum roll angle of 9^o and the pilot had to apply up to 46% of the lateral control to recover the attitude. In this case the pilot awarded a C severity rating.

6.2.3 Helicopter wake decay

Four induced velocity fields of the baseline wake and the wakes at 90%, 75% and 50% of the baseline wake strength were used in the level flight simulations. The results are shown in figure 20. The maximum roll angles caused by the wake at these four wake strengths are $45^o, 26^o, 15^o$ and 2^o, respectively. Compared with the baseline case, the wake at the 50% strength caused little upsets that almost no additional control was needed for recovery and a B rating was awarded. While at the 75% wake strength, up to 66% of the lateral control was require and resulted in an E rating. The required lateral control went to 70% at the 90% wake strength, in which case the pilot awarded it an F rating.

6.3 Wind turbine wake encounter

A modified Kocurek wind turbine wake model has been developed to simulate wind turbine wakes. It has been validated on the MEXICO wind turbine with the PIV wind tunnel measurements and the full CFD results [4]. The wind turbine wake model was applied to the WTN250 wind turbine, which has been installed near the East Midlands airport. The wind turbine wake encounter scenario is designed for a light aircraft (GA) approaching an airport, where a wind turbine is located nearby. On the approach to landing on the runway, the aircraft passes through the wind turbine wake field and is upset by the wake encounter. The severity of this encounter was also investigated using piloted flight simulations. Two wake encounter scenarios are shown in figure 21, where the crossing (90^o) and oblique (45^o) wake encounters are illustrated. The results of a typical wind turbine wake encounter simulation are shown in figure 22, where the aircraft dynamics and the pilot's controls were presented for the GA aircraft flew through the WTN250 wind turbine wake at the height of the wind turbine rotor center (100 ft) during the crossing encounter. In this case the wake generated minor upsets on the GA aircraft and a severity rating of B was awarded. This example demonstrates that the similar wake generation and flight simulation methodology of the helicopter wake encounter can be applied to study the wind turbine wake encounter.

7 CONCLUSION AND FUTURE WORK

Three different methods of modelling a helicopter wake, the prescribed wake model, free wake model and the CFD actuator disk model, have been developed and validated with wind tunnel experimental measurements and fly-by test data. The free wake model was selected to generate the wake vortices of a light helicopter based on a Dauphin configuration and hover taxing over an airport runway. The wake induced velocity fields were integrated into an aircraft flight dynamics model, which was developed in the FLIGHTLAB simulation package based on a Grob Tutor configuration and piloted flight simulations were carried out to study the severity of helicopter wake encounter on a light aircraft during landing.

Wake encounter parameters of helicopter height, forward speed, orientation angle and offset to the runway centerline were investigated in the simulations. In each simulation sortie, subjective pilot wake encounter severity rating and ob-

jective aircraft dynamic responses and pilot control activities were used to quantify the the effects of helicopter wake.

For this low attitude and relatively low forward speed hover taxing helicopter wake encounter scenario, the rotor wake is confined in the vicinity of helicopter. So in these preliminary simulations, the generated wake encounter upset is generally "mild" and the roll bank angle never exceeded the 30^o hazard criterion. However, in some test cases, the pilot rated the wake encounter as an F rating, which means, in his opinion, the safety of flight was compromised and hazard is intolerable. The reason that the pilot gave such a rating is because during the phase of landing the aircraft is close to the ground, where there is little room to manoeuvre the aircraft even the vortex upset is small. So the 30 degree bank angle criterion, which was developed for the high attitude and speed flight, might not be well suited for the wake encounter scenario during landing.

The simulations reveal that helicopter advance ratio, height, wake encountering orientation angle and offset to the centreline of runway all influence the encountering aircraft. This preliminary study suggests that for the current landing wake encounter scenario, where the helicopter is in low speed hover-taxing, the detectable horizontal distance is about three times the diameter of the rotor, which coincides with the current safety guideline of Civil Aviation Authority.

For the helicopter wake encounter during level flight, the vertical distance between the helicopter and the aircraft is an important parameter to determine the encounter severity. It was found that at a vertical distance of 2D, the wake still caused a rating C severity on the encountering aircraft. The simulations indicate that under the current test conditions the wake upsets reduced to insignificant levels after the wake was decayed to 50% of its full strength.

It is recognised that neither the number of the pilots nor the number of trials are sufficient in current wake encounter simulation study. Future simulation trials that include more test pilots have been planned.

Acknowledgements
The financial support from the Civil Aviation Authority (CAA) UK and the University of Liverpool is gratefully acknowledged.

REFERENCES

[1] T.S. Beddoes. A Wake Model for High Resolution Airloads. *U.S. Army/AHS Conference on Rotorcraft Basic Research*, February 1985.

[2] CAA. Aircraft accident report 1/93. Technical report, Civil Aviation Authority, 1993.

[3] CAA. CAP 493: Manual of Air Traffic Services Part 1. Technical Report 4, Civil Aviation Authority, November 2011.

[4] M. Carrion, R. Steijl, M. Woodgate, and G. Barakos. CFD Analysis of the Wake of the MEXICO Wind Turbine. *Wind Energy*, 00:1–17, 2012.

[5] H. H. Heyson. Analysis and comparison with theory of flow field measurements near a lifting rotor in the Langley full-scale tunnel. Technical Report NACA TN 3691, NASA, 1956.

[6] N.M. Komerath, Smith M, and C. Tung. A Review of Rotor Wake Physics and Modeling. *Journal of American Helicopter Society*, 56(2):1–19, 2011.

[7] F. Kopp. Wake vortex characteristics of military-type aircraft measured at airport Oberpfaffenhofen using the DLR Laser Doppler Anemometer. *Aerospace Science and Technology*, (4):191–199, 1999.

[8] G. Leishman. *Principles of helicopter aerodynamics*. Cambridge aerospace series book, Cambridge, UK, second edition, 2007.

[9] J.G. Leishman, M.J. Bhagwat, and A. Bagai. Free-Vortex Filament Methods for the Analysis of Helicopter Rotor Wakes. *Journal of Aircraft*, 39(5):759–775, 2002.

[10] G.D. Padfield, B. Manimala, and G.P. Turner. A Severity Analysis for Rotorcraft Encounters with Vortex Wakes. *Journal of American Helicopter Society*, 49(4):445–456, 2004.

[11] G.D. Padfield and M.D. White. Flight simulation in academia - heliflight in its first year of operation at the university of liverpool. *The Aeronautical Journal*, 107(1075):529–538, 2003.

[12] R. Steijl and G.N. Barakos. Sliding mesh algorithm for CFD analysis of helicopter rotor-fuselage aerodynamics. *International Journal for Numerical Methods in Fluids*, 58(5):527–549, 2008.

[13] S. Teager, K. Biehl, L. Garodz, J. Tymczyszym, and D. Burnham. Flight test investigation of rotorcraft wake vortices in forward flight. Technical Report DOT/FAA/CT-94/117, FAA, 1996.

[14] P. Wilson and S Lang. Technical Report to Support the Safety Case for Recategorization of ICAO Wake Turbulence Standards: Proposed wake turbulence catagories for all aircraft commonly provided with air traffic service. Technical Report 0, EUROCONTROL and FAA, April 2011.

[15] P. Wilson, C Lepadatu, S Barnes, and S Lang. Technical Report to Support the Safety Case for Recategorization of ICAO Wake Turbulence Standards: An Overview of Key Aviation Accidents Sometimes Assumed to Have Been Casued by Wake Turbulence. Technical Report 0.1, EUROCONTROL and FAA, December 2010.

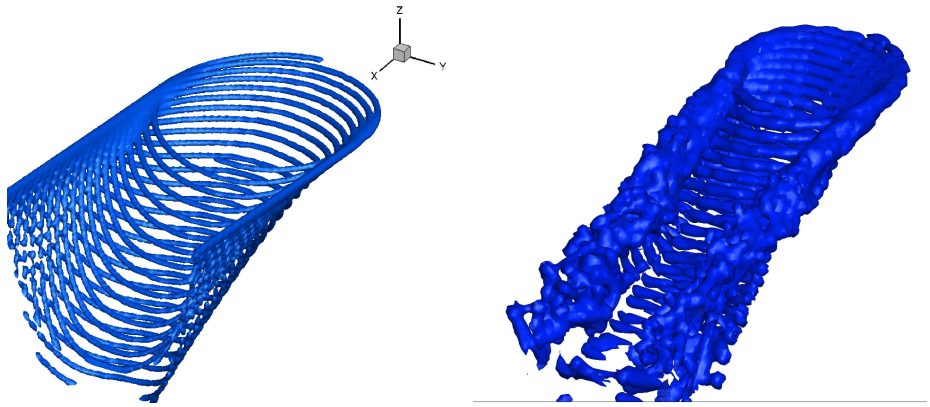

(a) Prescribed wake model (b) Free wake model

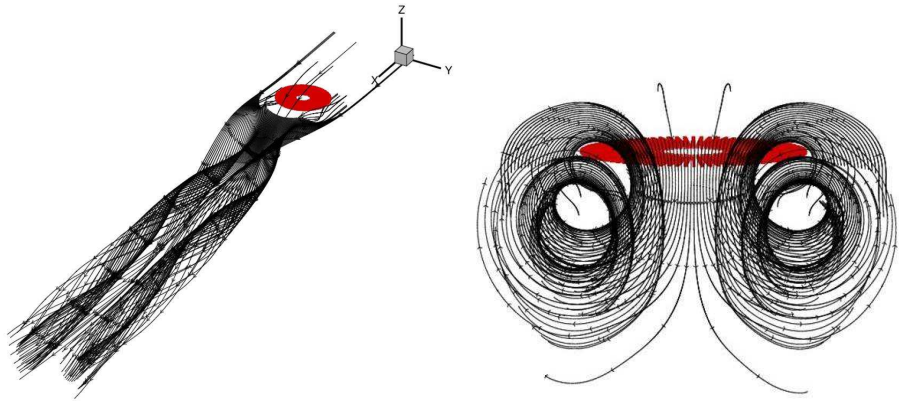

(c) AD model (d) AD model

Figure 1: Wake vorticity iso-surface plots of the prescribed wake (Beddoes) model and the free wake model and the wake stream-trace plots of the actuator disk model of a light helicopter with 4-bladed rotor, C_t=0.013 and μ=0.1.

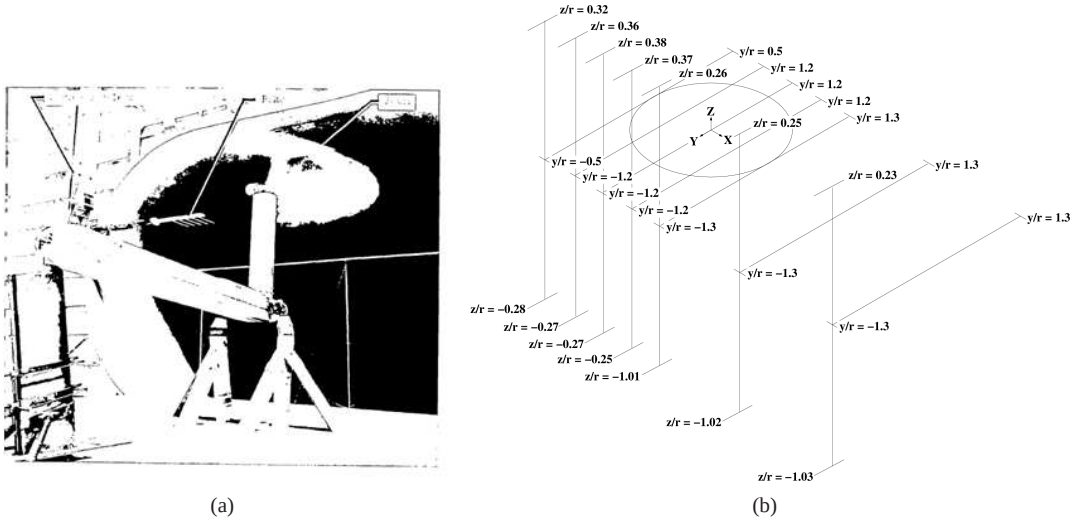

(a) (b)

Figure 2: Heyson's wind tunnel rotor wake test set-up and the positions of velocity measurement planes

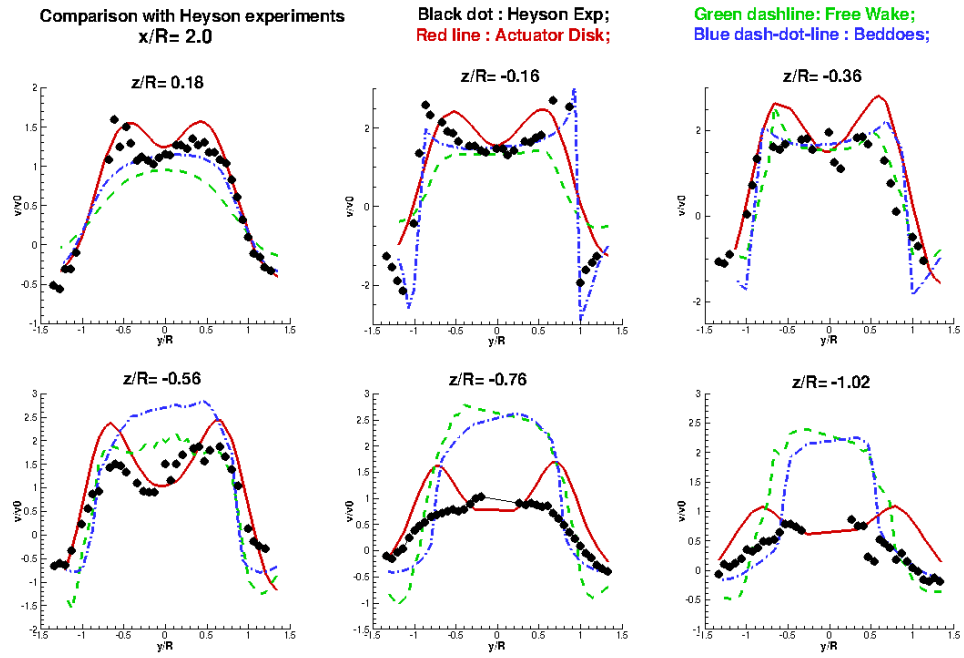

(a) x/R=2.0

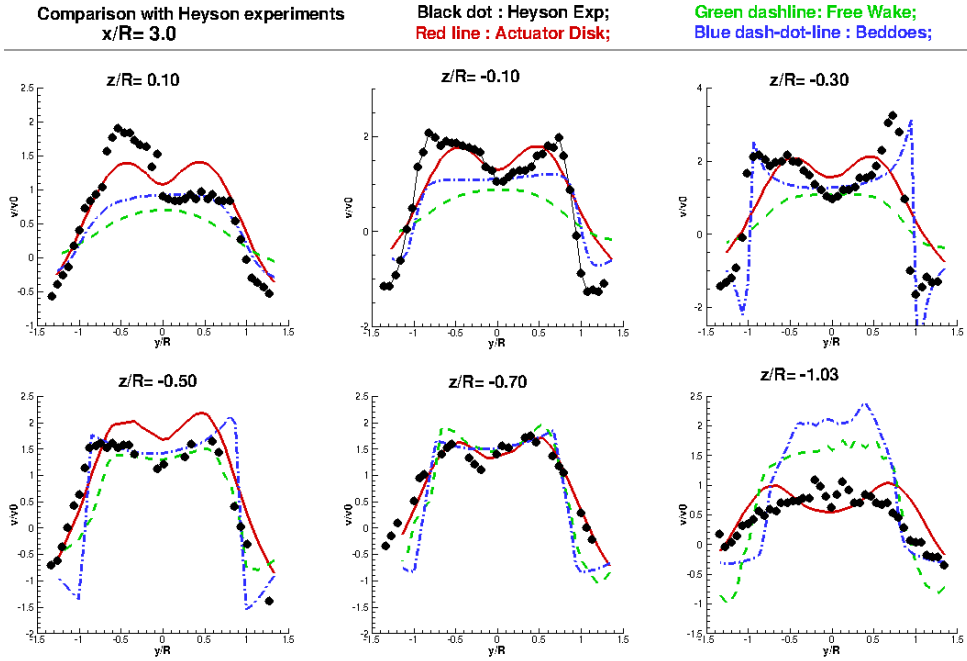

(b) x/R=3.0

Figure 3: Comparison of three wake models against Heyson's experiments [5] at x/R=2 and $x/R = 3$ planes, C_t=0.0064 and μ=0.095.

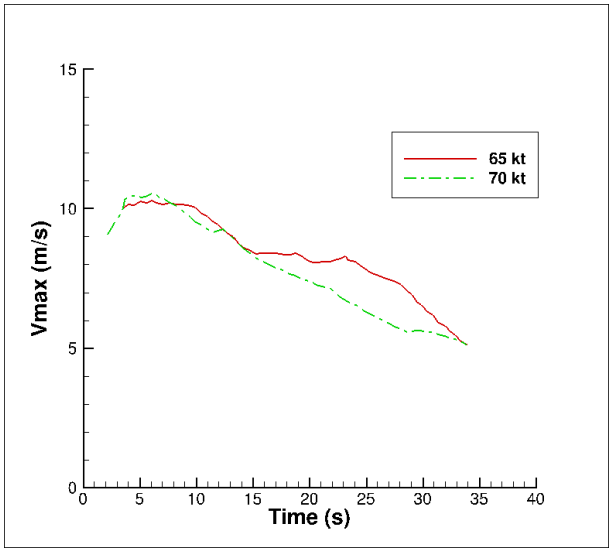

Figure 4: Maximum tangential velocity versus vortex age [7], LIDAR measurements on a forward flying Puma helicopter with speeds of 65 kt (run 13/01) and 70 kt (run 19/07).

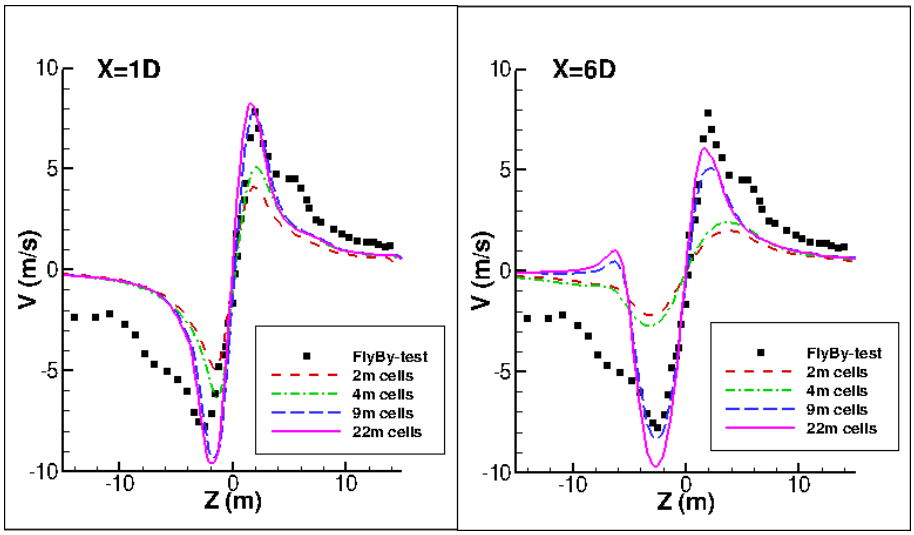

(a) CFD actuator disk model

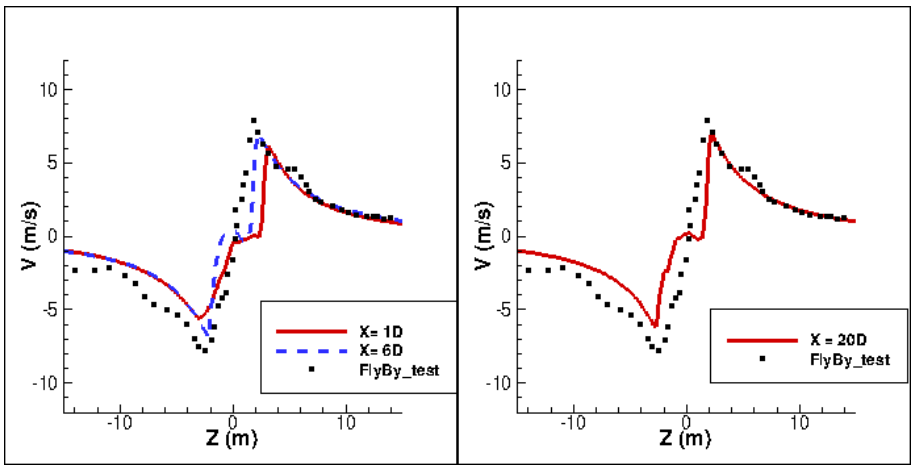

(b) Beddoes wake model with the measured decay relation

Figure 5: Maximum tangential velocity distributions at different downstream positions predicted by Beddoes wake model with the measured decay relation, Puma helicopter with forward speed of 65 kt.

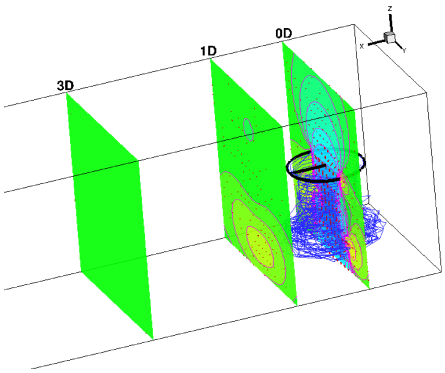

(a) μ=0.0

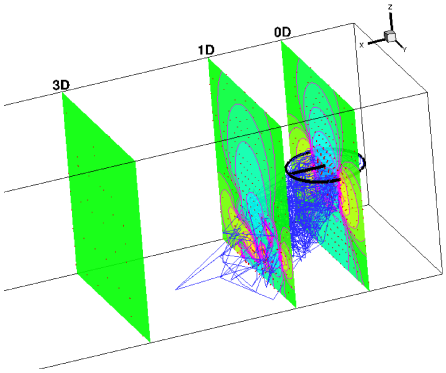

(b) μ=0.05

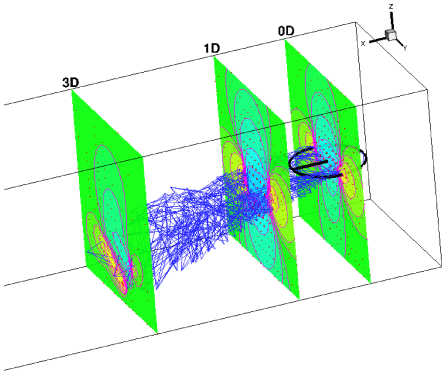

(c) μ=0.1

Figure 6: Induced velocity fields generated by the free wake model for a Dauphin rotor at different advance ratios, C_t=0.013, h=50 ft.

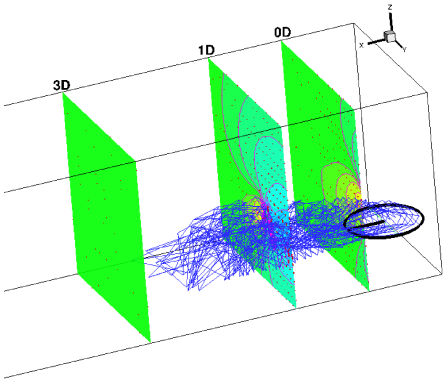

(a) Angle =45^o, Offset=2D, h=50 ft

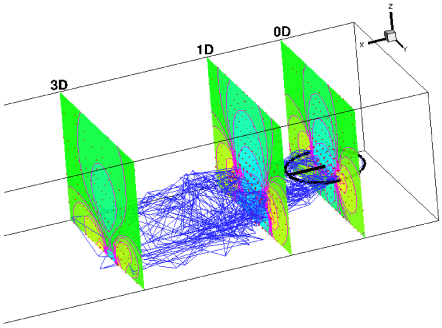

(b) h=20 ft

Figure 7: Induced velocity fields generated by the free wake model for a Dauphin rotor C_t=0.013, μ=0.1.

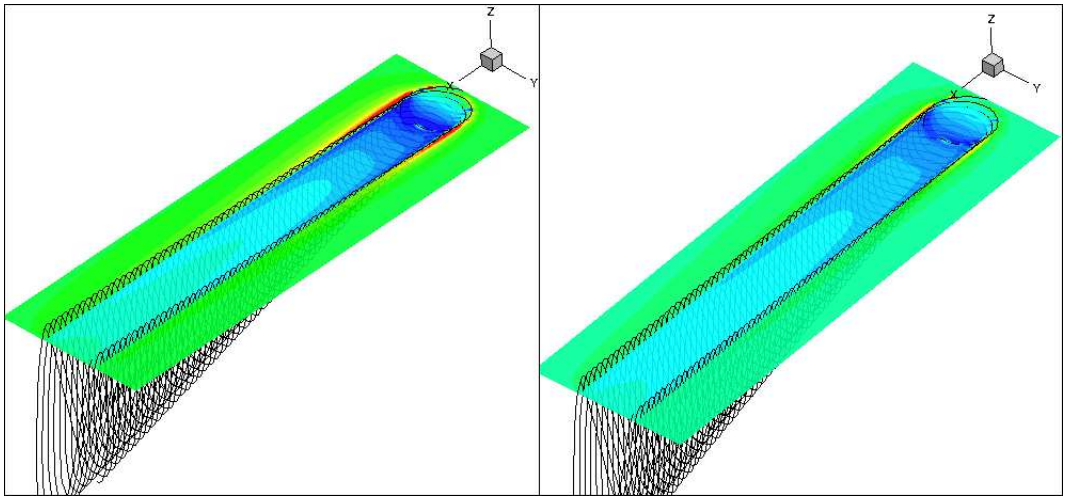

Figure 8: Induced velocity fields generated by the Beddoes wake model for a Dauphin rotor at height of 200 ft, C_t=0.013, μ=0.15, baseline (no decay) and 50% wake decay.

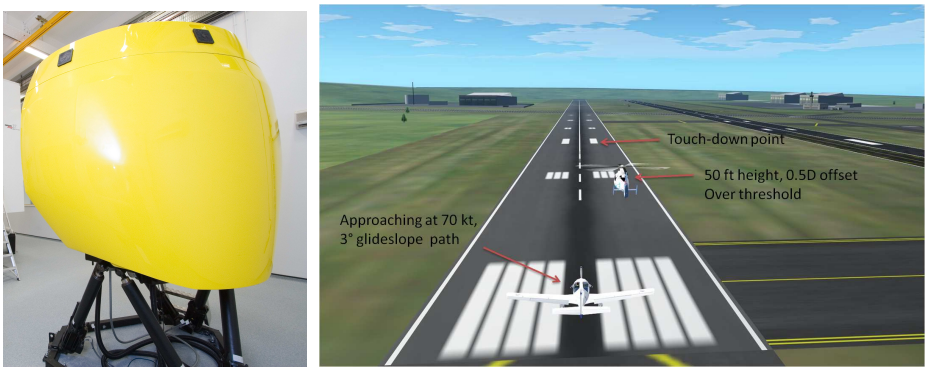

(a) HELIFLIGHT simulator (b) Simulation scene

Figure 9: HELIFLIGHT simulator and the wake encounter simulation scene.

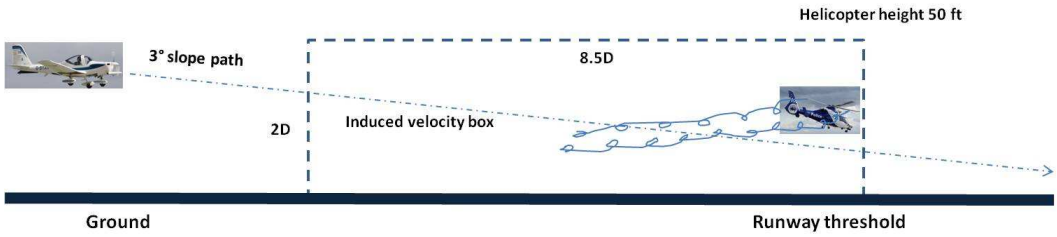

Figure 10: Schematic of the GA aircraft flight path and wake encounter.

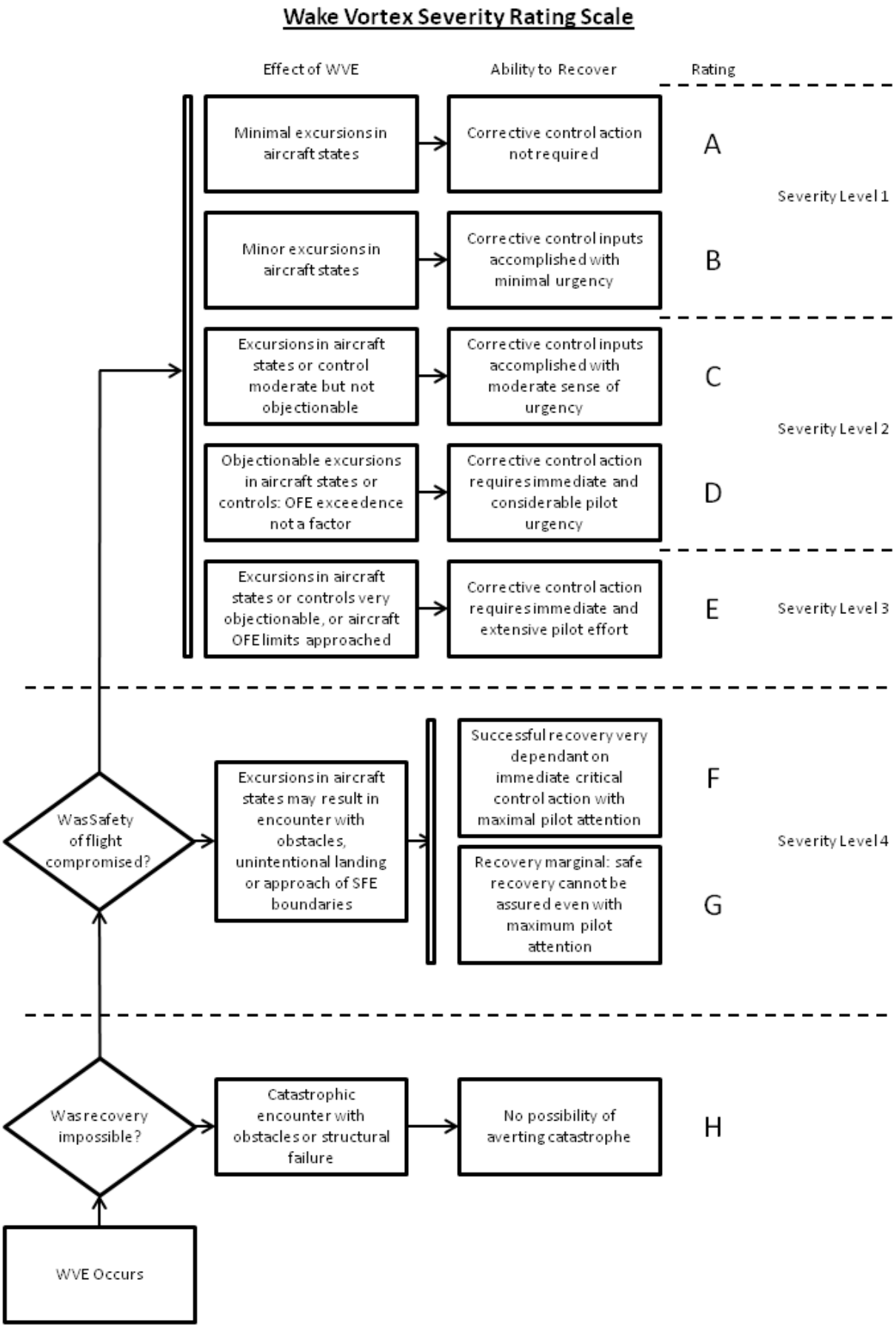

Figure 11: Pilot wake encounter severity rating scale [10].

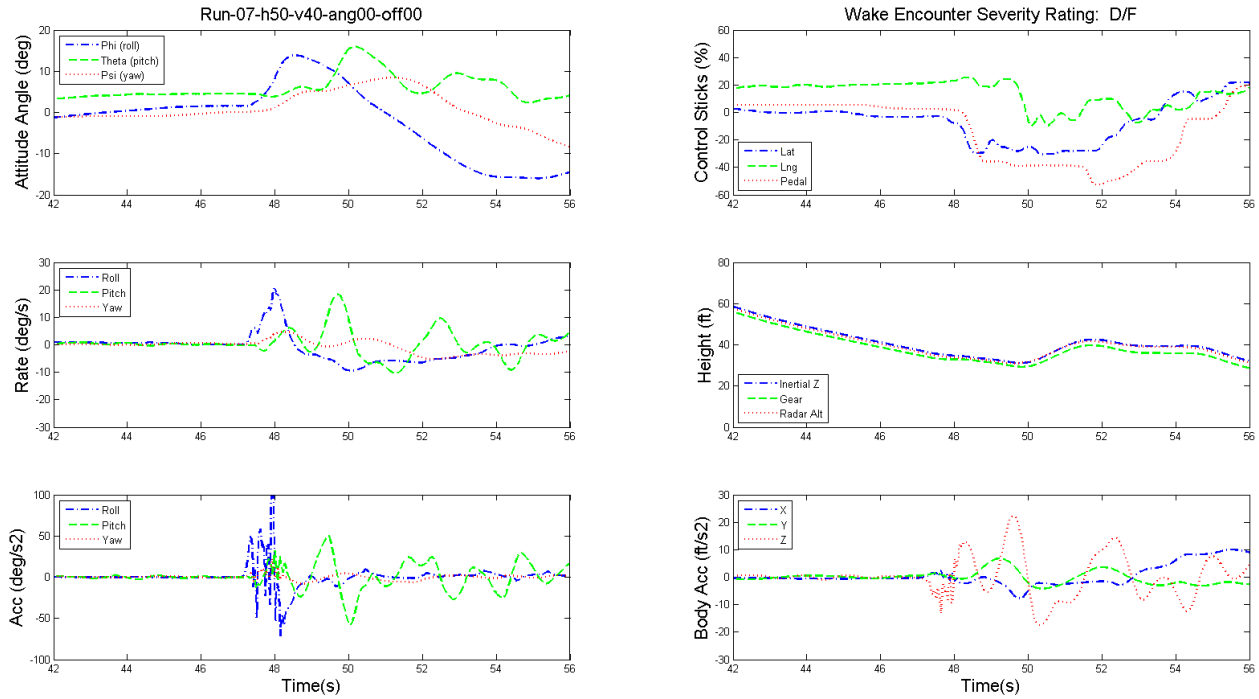

Figure 12: Time history of the dynamics of GA aircraft and pilot's controls during wake encounter,h=50 ft, μ=0.1, angle=0^o, offset=0.

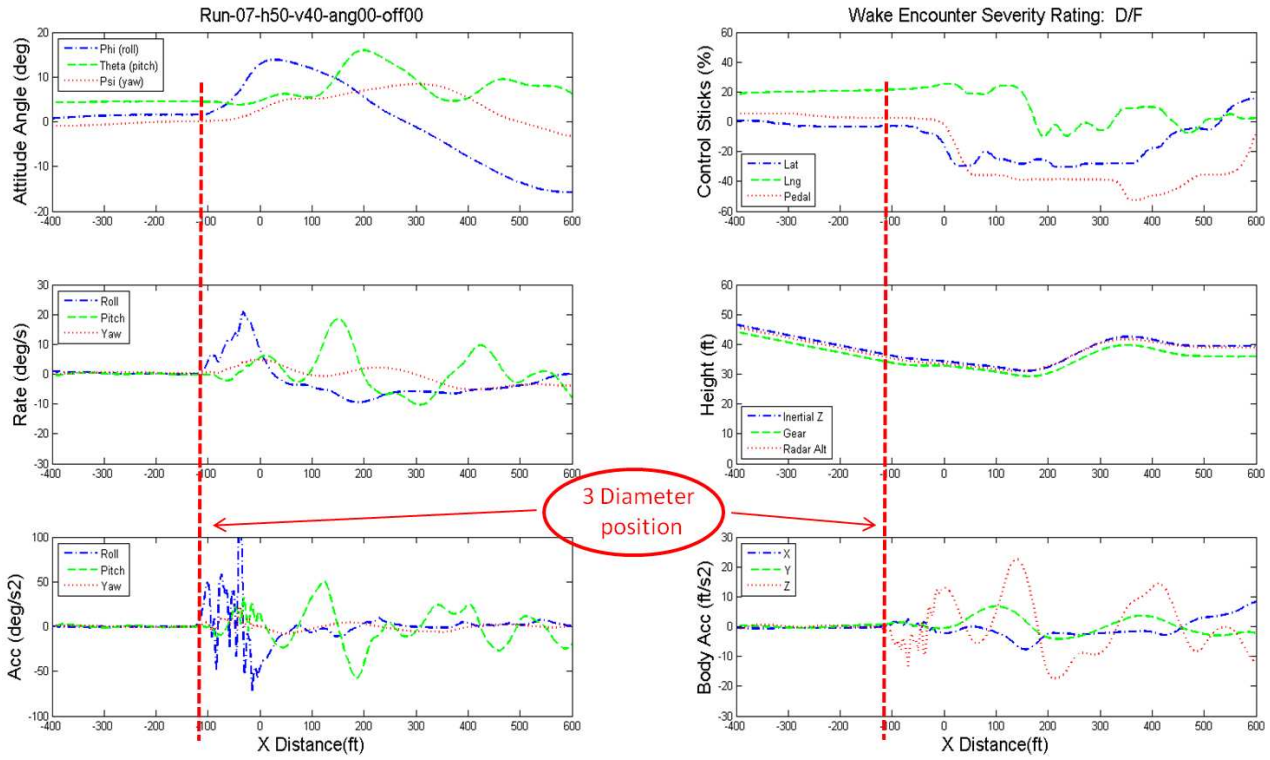

Figure 13: Dynamics of GA aircraft and pilot's controls during wake encounter, h=50 ft, μ=0.1, angle=0, offset=0.

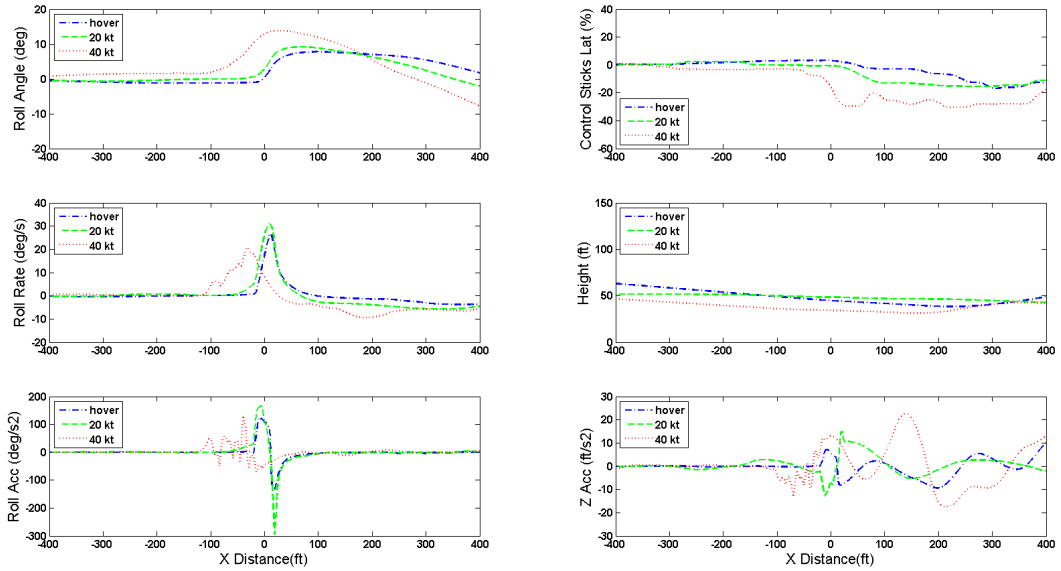

Figure 14: Dynamics of GA aircraft and pilot's controls during wake encounter, h=50 ft, speed= 0, 20 kts, 40 kts, angle=0^o, offset=0.

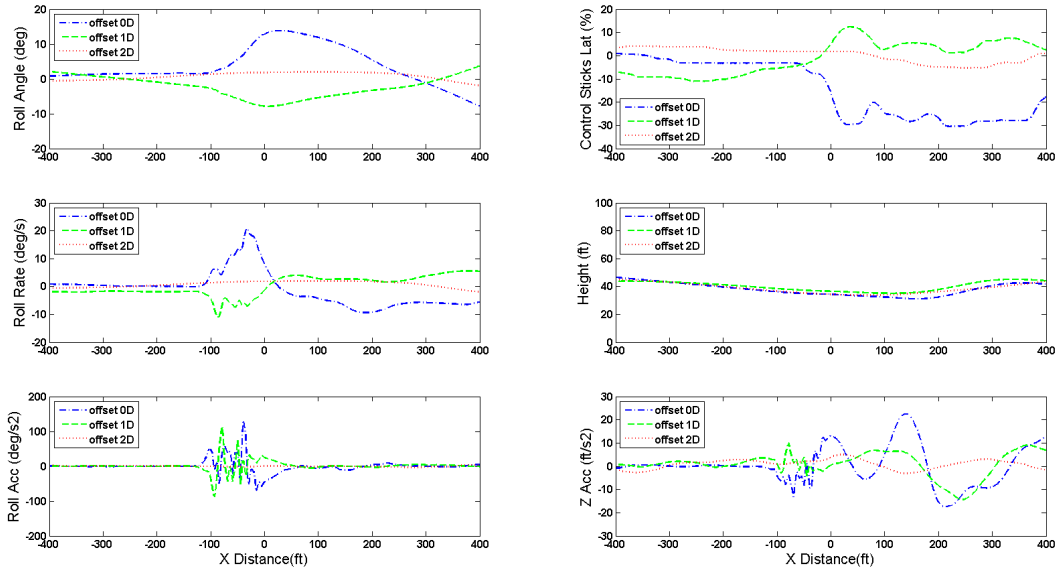

Figure 15: Dynamics of GA aircraft and pilot's controls during wake encounter, h=50 ft, μ=0.1, angle=0^o, offset=0, 1D, 2D.

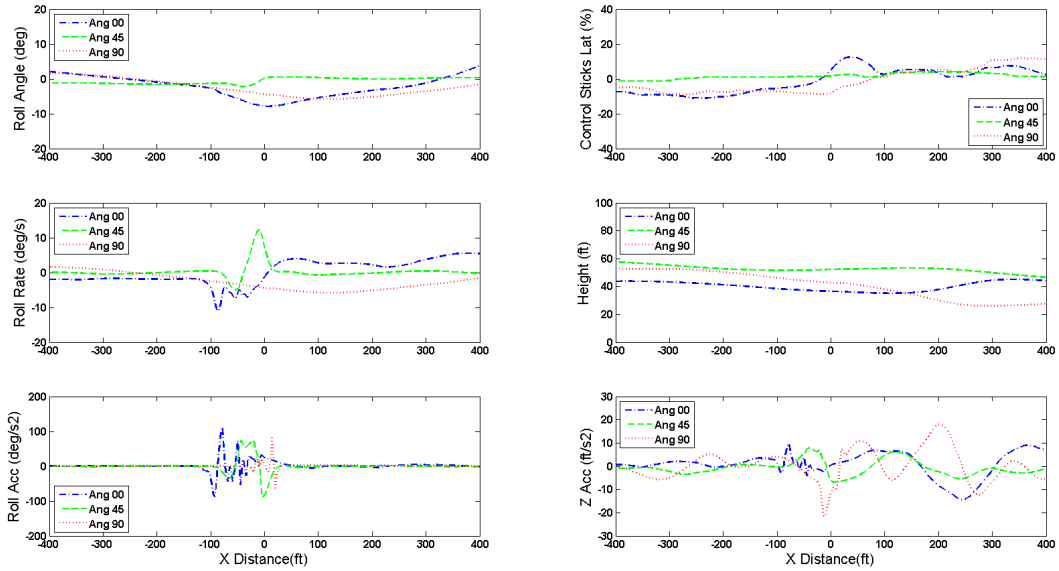

Figure 16: Dynamics of GA aircraft and pilot's controls during wake encounter, h=50 ft, μ=0.1, angle=0^o, 45^o, 90^o. offset=1D.

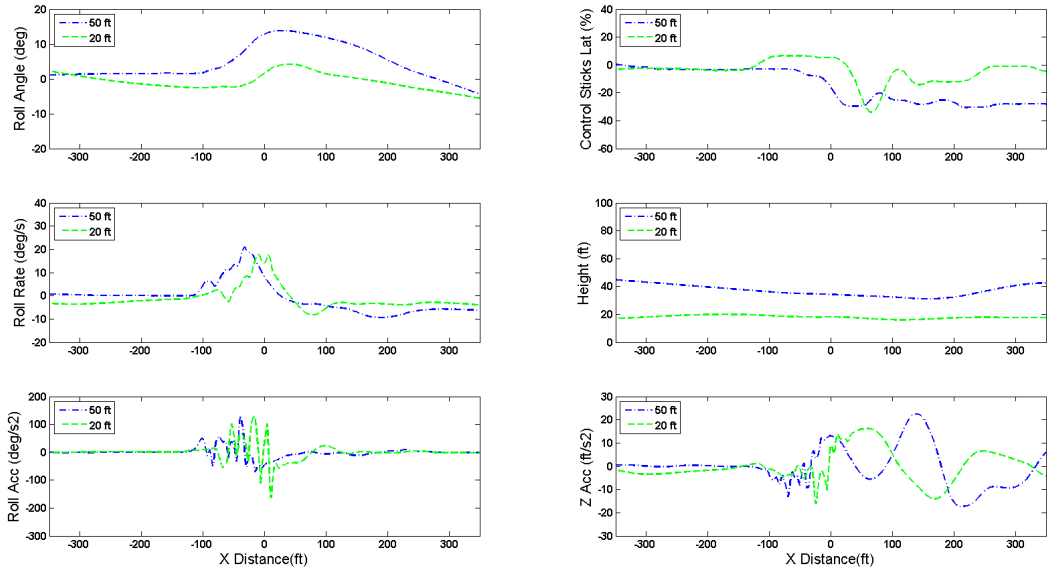

Figure 17: Dynamics of GA aircraft and pilot's controls during wake encounter, helicopter μ=0.1, angle=0^o, offset=0, h=50 ft, 20 ft.

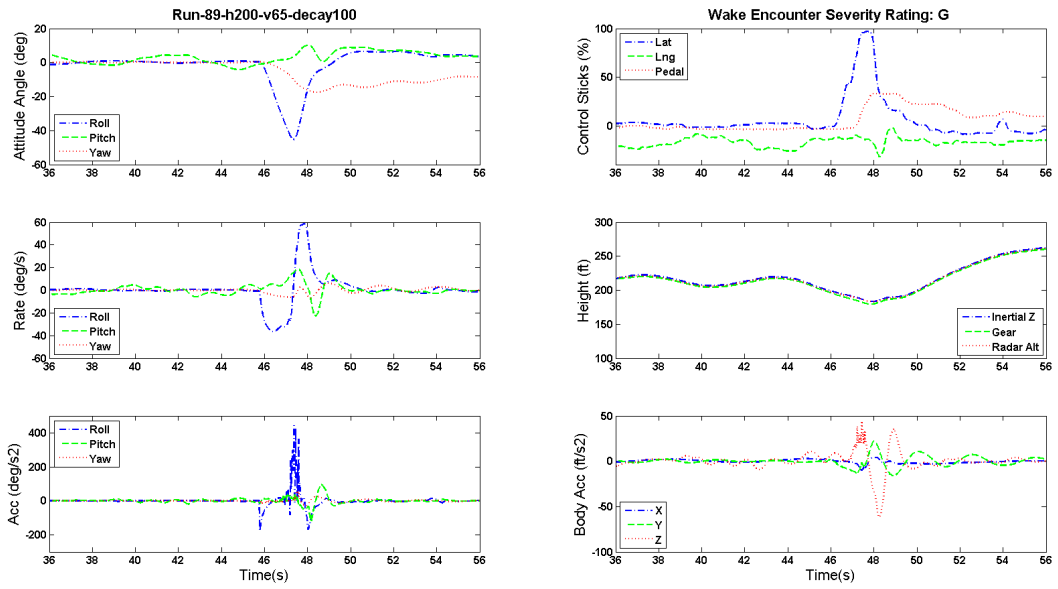

Figure 18: Dynamics of GA aircraft and pilot's controls during level flight wake encounter, h=200 ft, μ=0.15.

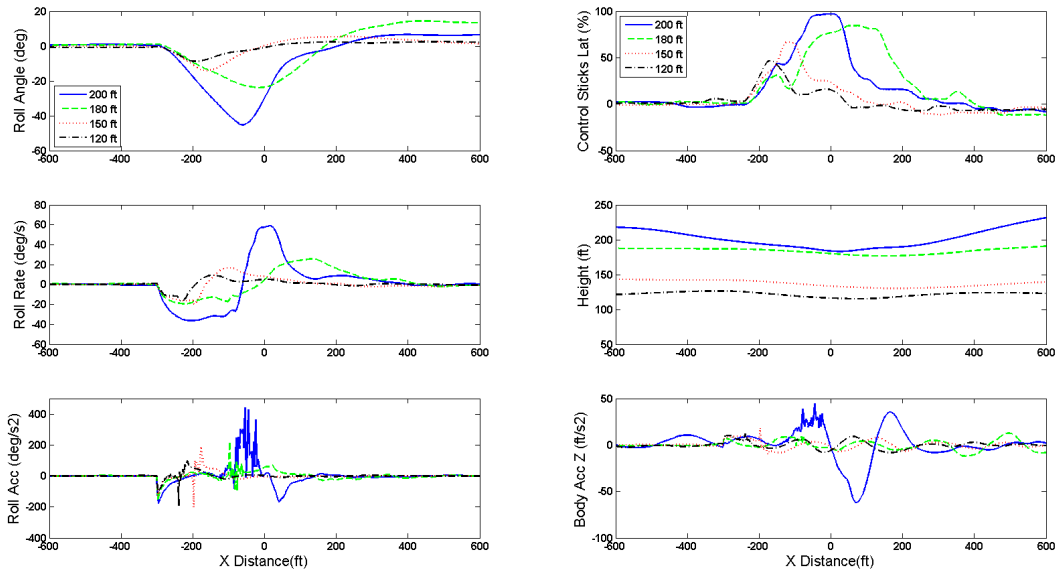

Figure 19: Dynamics of GA aircraft and pilot's controls during level flight wake encounter, h= 200 ft, μ=0.15, GA aircraft altitude = 200 ft, 180 ft, 150 ft and 120 ft.

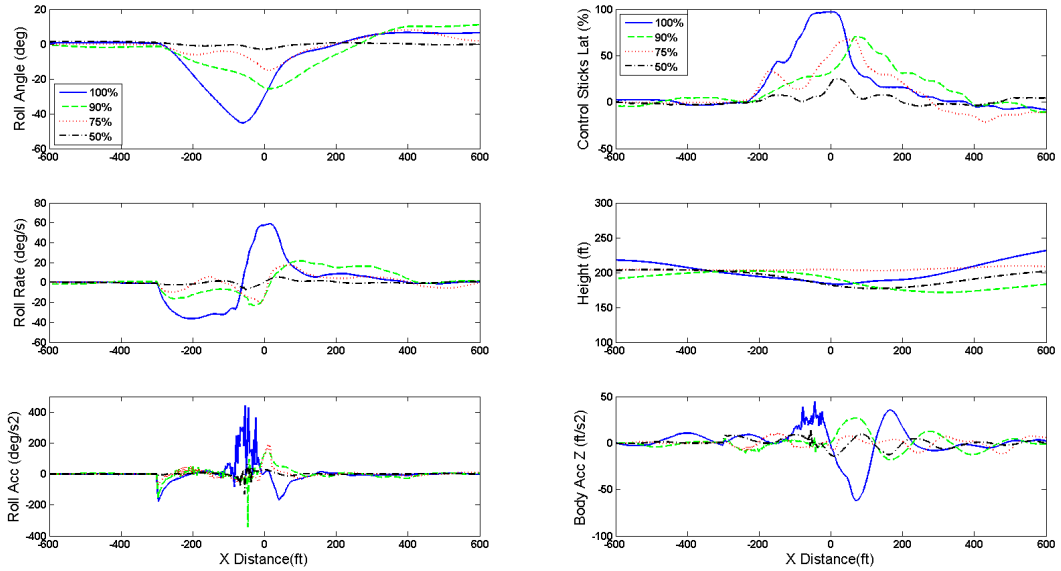

Figure 20: Dynamics of GA aircraft and pilot's controls during level flight wake encounter, h=200 ft, μ=0.15, wake decay 100%, 90%, 75% and 50%.

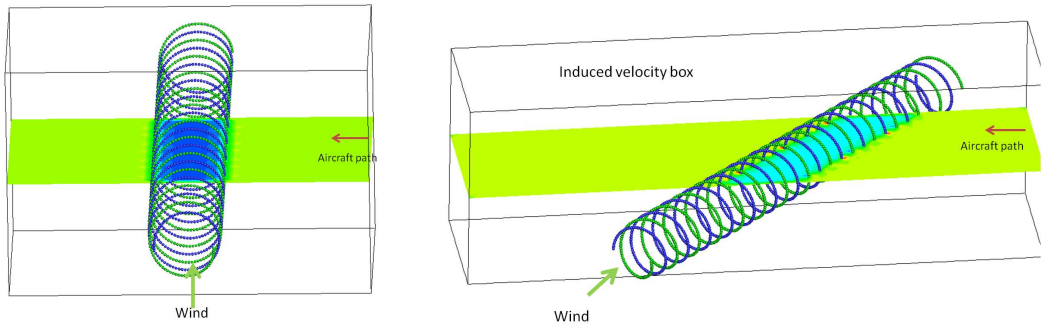

(a) Crossing encounter (b) Oblique encounter

Figure 21: Wind turbine wake geometry and the contour plots of the induced velocity for the crossing and oblique wind turbine wake encounters

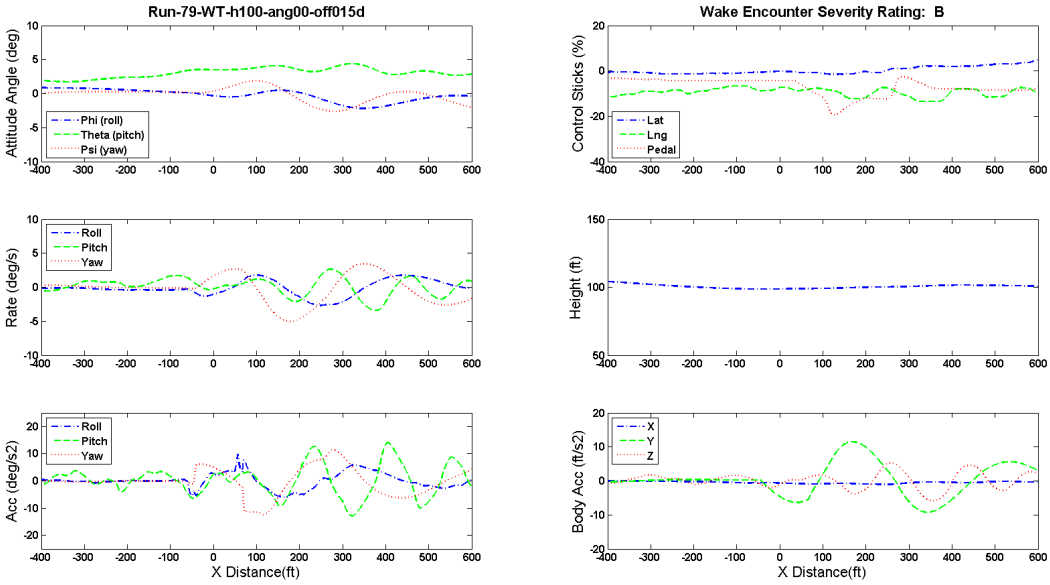

Figure 22: Dynamics of GA aircraft and pilot's controls during WTN250 wind turbine wake encounter, Crossing encounter, height of wind turbine rotor center 100 ft, wind speed 10 m/s, GA altitude 100 ft.